

Enhancing the frequency regulation performance of coal-fired power plants under deep peak shaving conditions by coupling external heat into the regenerative systems[#]

Peng Wang, Chaoyang Wang*, Ming Liu, Weixiong Chen, Junjie Yan

State Key Laboratory of Multiphase Flow in Power Engineering, Xi'an Jiaotong University, Xi'an 710049, China

chaoyang.wang@xjtu.edu.cn

ABSTRACT

With the increasing penetration of intermittent renewable energy sources in the power generation system, coal-fired power plants have to operate in deep peak shaving conditions frequently. Since the frequency regulation capability of coal-fired power plants under low load conditions is limited, increasing the load cycling rate is necessary, and coupling external heat storage to the thermal system to enhance the transient response rate is a good choice. This paper established and validated a dynamic model of a 660 MW ultra-supercritical coal-fired power plant. The transient performance of the power unit during load cycling was simulated and analyzed based on the dynamic model. Therminol VP-1 was used as the thermal source to release heat to the water via an oil-water heater during the power plant loading up from 30% to 50% THA. When the feedwater output temperature remains unchanged, the amount of steam extracted by the high-pressure heater will be reduced, and the output power of the turbine unit can be increased. The simulation results show that the load cycling rate of coal-fired power generation under the peak shaving conditions can be improved from 2.2% to 3.5% $P_e \text{ min}^{-1}$. At a load cycling rate of 2.0% $P_e \text{ min}^{-1}$ and a Therminol VP-1 flow rate of 100 kg s^{-1} , the coupled thermal storage system reduces the maximum relative deviation of the output power by 11.8% and improved the whole plant thermal efficiency difference by 0.15%.

Keywords: thermal energy storage, load cycling rate, deep peak-shaving, oil-water heater, Therminol VP-1

NONMENCLATURE

Abbreviations

TES	Thermal energy storage
CFPP	Coal-fired power plant
RH	Reheater

SH	Superheater
ECO	Economizer
HP	High-pressure cylinder
IP	Intermediate-pressure cylinder
LP	Low-pressure cylinder
LHV	Lower heating value of coal
<i>Symbols</i>	
$R_{p,w}$	Relative deviation of output power
$R_{p,s}$	Relative deviation of live steam pressure
V_e	Load cycling rate
T_{ls}	Live steam temperature
T_{rh}	Reheat steam temperature
P	Output power
P_e	Nominal load
p_0	Live steam rated pressure
B	Coal feed rate

1. INTRODUCTION

Increasing the proportion of renewable energy in the power supply structure is of crucial importance when facing global warming and the energy crisis. However, due to the unstable and discontinuous characteristics of wind, solar, and other renewable energy, coal-fired power plants (CFPPs) must operate frequently under peak shaving conditions for flexible load output and to maintain the power grid's real-time power balance [1].

However, in low-load work conditions, the flexibility of CFPP is seriously decreased due to insufficient heat storage and the flowing fluid of the boiler. Especially during the loading-up process, the heating of the boiler is usually increased by elevating the amount of coal feed. Even though a time and distance gap existed between the coal feed and heating of the boiler, it failed to catch up on real-time heat requirements.

The insufficiency in heat can be solved by coupling the thermal energy storage (TES) system to CFPP, which provides additional feedwater heat externally, solving

[#] This is a paper for the 16th International Conference on Applied Energy (ICAE2024), Sep. 1-5, 2024, Niigata, Japan.

the problem of insufficient heat during the loading-up process. This measure facilitates the decoupling of power generation temporally and spatially, improving the operational flexibility of CFPPs [2].

Many scholars have studied methods for thermal energy storage to adjust the power generation of CFPPs.

onal flexibility and thermal efficiency of the thermal power system. Li et al. [4] studied and compared three charging strategies and two discharging strategies for integrating High-Temperature Thermal Storage into the thermal power plant steam-water cycle and found all of the strategies can improve the dynamic response speed of CFPPs. Trojan et al. [5] studied the installation of a hot water storage tank to improve the flexibility of a 200 MW power plant, increasing the maximum load of the generator set by 15 MW and reducing the minimum load by 21.96 MW. Ding et al. [6] proposed a steam accumulator integrated with a steam turbine bypass system, which increased the loading up rate of 660 MW supercritical CFPP from 1.5% to 3.0% Pe min^{-1} within the range of 40% to 50% THA.

Most existing heat storage systems use molten salt and steam as heat transfer fluids. Some scholars have studied and compared the performances of different heat transfer fluids. Gerard et al. [7] made theoretical and experimental comparisons on the performances of two heat transfer fluids, thermal oil Therminol VP-1 and silicone fluid Syltherm 800, in heat exchangers. The results showed that under the same operating conditions, Therminol VP-1 has higher heat transfer efficiency and lower thermal losses. Nabeel et al. [8] studied the thermal properties of three heat exchange fluids, water, Therminol VP-1, and molten salt Solar salt. The research showed that Solar salt was the best choice under temperatures higher than 600 K. However, in the middle temperature ranging between 320 K and 575 K, Therminol VP-1 has better thermal performance. For the heat exchanger in this paper, the heat exchange fluid is used to heat feedwater, and the working range mainly focuses between 400 K - 600 K. Thus, VP-1 is a preference under this condition.

It can be seen that, in the medium-temperature region, heat transfer thermal oil is an ideal heat transfer fluid. However, at present, research on thermal oil is limited to performance, and few cases have been published about applying thermal oil to the TES system as heat transfer fluid.

Therefore, this paper intended to couple the TES system in the feedwater bypass of CFPP and to provide heat to feedwater through the oil-water heater during the CFPP loading up, from 30% to 50% THA. The dynamic

Zhang et al. [3] proposed a molten salt heat storage system based on the integration of multiple heat sources (high-temperature flue gas and superheated steam) in CFPPs. During the heat storage process, the minimum load of CFPP is reduced from 30% to 14.5% THA, which improves the operati

characteristics and the whole plant thermal efficiency difference of CFPP during the loading up dynamic process after coupling the TES system are discussed. By this means, we aim to provide additional heat to CFPP to solve the problem of insufficient heat supply from the boiler during the loading-up process. Ultimately, the operation flexibility and stability of CFPP can be improved.

2. SYSTEM DESCRIPTION

This paper selects a 660 MW ultra-supercritical CFPP located in Inner Mongolia, China, as the research object. A simulation model of the CFPP is established, and a TES system is coupled to the feedwater bypass.

2.1 Coupled TES system in CFPP

As shown in *Fig. 1*, the boiler feedwater in the original CFPP structure is heated to live steam by an economizer (ECO) and superheater (SH). Then, it enters the high-pressure cylinder (HP) to do work, and the steam after work is heated by a reheater (RH) to become reheated steam. The reheated steam enters the intermediate-pressure cylinder (IP) and the low-pressure cylinder (LP) to do work. After work, the steam becomes condensed water, which passes through the condenser, heater, and deaerator and finally becomes the boiler feedwater into the boiler. Complete the CFPP cycle. The parameters of CFPP under 100%THA condition are listed in Table 1.

As shown in *Fig. 2*, during low electricity demand and CFPP loading down process, Cycle 2 operates with the outlet gas from the low-temperature SH serving as the heat source to heat Therminol VP-1 via an oil-flue gas heater. The heated Therminol VP-1 is stored in the high-temperature storage tank, and after the heat stored in the flue gas is released, the flue gas is returned to the ECO inlet. During the process of high electricity demand and loading up, Cycle 1 is operated, and Therminol VP-1 in the thermal storage tank enters the oil-water heater to exchange heat with the bypass feedwater, the heated feedwater enters the boiler feedwater, and Therminol VP-1 enters the low-temperature storage tank.

At this time, the amount of steam extracted from the HP and IP is reduced, and more extracted steam is

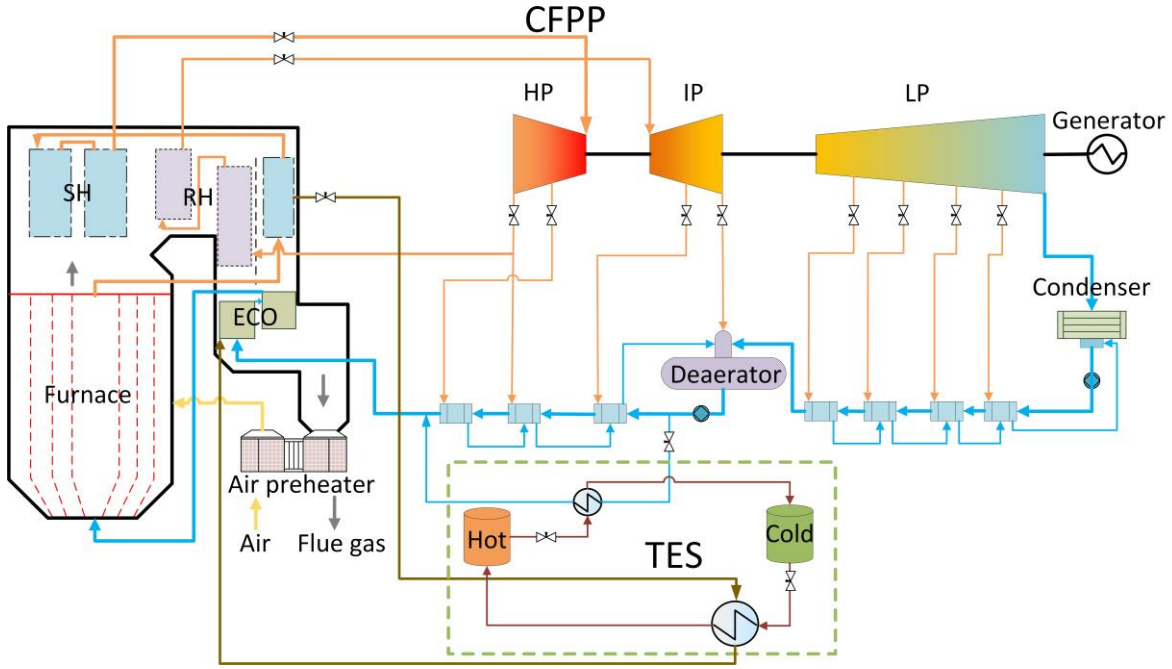


Fig. 1 Coupled the TES system in CFPP

returned to the turbine to expand and do work, which is conducive to the rapid increase of CFPP's output power.

Table 1 The parameters of CFPP

Items	Units	Value
Lower heating value of coal	$\text{kJ}\cdot\text{kg}^{-1}$	18520
Coal feed rate	$\text{kg}\cdot\text{s}^{-1}$	78.5
Live steam pressure	MPa	28.0
Live steam temperature	$^{\circ}\text{C}$	600
Reheat steam temperature	$^{\circ}\text{C}$	620
Feedwater flow rate	$\text{kg}\cdot\text{s}^{-1}$	511.9

viscosity in the lower temperature range and may be used as a thermal oil. Table 2 displays the thermal physical property characteristics in this temperature range.

Table 2 Physical properties of Therminol VP-1 [9]

Parameters	Property equation
$c_p/\text{J}\cdot\text{kg}^{-1}\cdot\text{K}^{-1}$	$2.82T+716$
$\lambda/\text{W}\cdot\text{m}^{-1}\cdot\text{K}^{-1}$	$1.73\times 10^{-7}T^2+7.62\times 10^{-6}T+0.14$
$\rho/\text{kg}\cdot\text{m}^{-3}$	$-7.61\times 10^{-4}T^2-2.24\times 10^{-1}T+1191$
$\mu/\text{N}\cdot\text{s}\cdot\text{m}^{-2}$	$(-2.3\times 10^{-5}T^3+5.61\times 10^{-3}T^2-19.89T+1822)^{-1}$

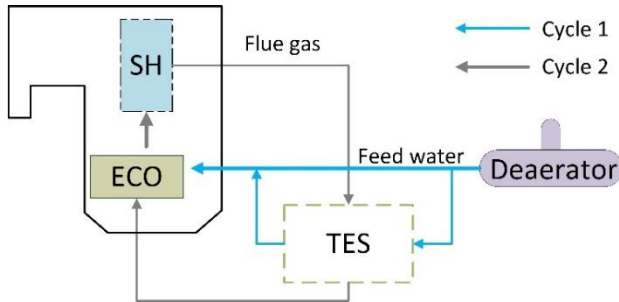


Fig. 2 Circulation diagram of the TES system

2.2 Therminol VP-1 physical properties

Therminol VP-1 is a eutectic mixture of 26.5% biphenyls and 73.5% diphenyl others. It is a synthetic heat transfer oil with outstanding thermal stability and low viscosity. Over a broad temperature range of 285 K – 673 K, it can deliver efficient, dependable, and constant performance. Therminol VP-1 maintains a very low

2.3 Indexes for transient performances

2.3.1 Load cycling evaluation indicators

A load cycling evaluation approach is proposed to enhance the grid-connected units' peak and frequency regulation performance. The evaluation indicators include ramp rate indicator K_1 , adjustment accuracy indicator K_2 , response time indicator K_3 , and comprehensive performance indicator K_p .

The climbing rate indicator K_1 :

$$K_1 = 2 - \frac{V_{e,s}}{V_e} \quad (1)$$

where $V_{e,s}$ is the standard ramp rate, Pe min^{-1} , for fossil fuel power plants with the pulverized coal boiler, $1.5\% \text{ Pe min}^{-1}$ is mandatory. V_e is the actual ramp rate, Pe min^{-1} .

The adjustment accuracy indicator K_2 :

$$K_2 = 2 - \frac{\Delta W_a}{\Delta W_s} \quad (2)$$

$$\Delta P = P_{\text{set}} - P \quad (3)$$

$$\Delta W_a = \frac{\int_{\tau_1}^{\tau_2} |\Delta P| d\tau}{\tau_2 - \tau_1} \quad (4)$$

where ΔW_s is the standard adjustment accuracy, MW, for fossil fuel power plants with the pulverized coal boiler, $1.0\% \text{ Pe min}^{-1}$ is mandatory. ΔW_a is the actual adjustment accuracy, MW. ΔP is the real-time power deviation, MW; P is the real-time output power, MW; P_{set} is the set value of output power, MW; τ_1 is the time when real-time generated power reaches the dead area of the load target, s; τ_2 is the time when the current load cycling process is completed, s.

The response time indicator K_3 :

$$K_3 = 2 - \frac{\Delta \tau_a}{\Delta \tau_s} \quad (5)$$

$$\Delta \tau_a = \tau_z - \tau_0 \quad (6)$$

where $\Delta \tau_s$ is the standard response time, s, for fossil fuel power plants with the pulverized coal boiler, 60 s is mandatory. $\Delta \tau_a$ is the actual adjustment accuracy, s. τ_0 is the delivery time of load instructions, s. τ_z is the time when real-time generated power steps out of the dead area of initial output power, s.

The comprehensive performance indicator K_p :

$$K_p = K_1 \times K_2 \times K_3 \quad (7)$$

2.3.2 Relative deviation of output power and live steam pressure

During the CFPP loading-up process, some parameters can reflect the stability and flexibility of the dynamic process. The relative deviation of output power can represent the stability of CFPP output power, and its mathematical formula is as follows:

$$R_{p,w} = \left| \frac{\Delta P}{P_e} \right| \times 100\% \quad (8)$$

where $R_{p,w}$ is the relative deviation of output power, MW; P_e is the rated load, 660 WM.

The relative deviation of live steam pressure can represent the stability of live steam pressure, and its mathematical formula is as follows:

$$R_{p,s} = \left| \frac{\Delta p}{p_0} \right| \times 100\% \quad (9)$$

$$\Delta p = p_{\text{set}} - p \quad (10)$$

where $R_{p,s}$ is the relative deviation of live steam pressure, and p is the real-time value of live steam pressure. p_{set} is the set value of live steam pressure, MPa; p_0 is the rated pressure of live steam, MPa.

2.3.3 Dimensionless cumulative deviation of output power and live steam pressure

ΔP_{all} is the dimensionless cumulative deviation of the output power during the loading up process, MW, and the mathematical formula is:

$$\Delta P_{\text{all}} = \int_{\tau_y}^{\tau_z} \frac{|\Delta P|}{P_e} d\tau \quad (11)$$

Δp_{all} is the dimensionless cumulative deviation of the live steam pressure during the loading up process, MPa, as follows:

$$\Delta p_{\text{all}} = \int_{\tau_y}^{\tau_z} \frac{|\Delta p|}{p_0} d\tau \quad (12)$$

2.3.4 Energy consumption analysis

The whole plant thermal efficiency is also the most comprehensive metric for considering CFPPs, reflecting both the extent to which CFPPs utilize the heat of the fuel and the energy conversion rate at which heat is converted to electricity. Determining the whole plant thermal efficiency for the entire process of the load cycle is the key to analyzing the economics of a CFPP.

The formula for the whole plant thermal efficiency is as follows.

$$\eta_{\text{cp}} = \frac{\int_{\tau_0}^{\tau_z} P d\tau}{\int_{\tau_0}^{\tau_z} B d\tau \times \text{LHV} + Q_o} \times 100\% \quad (13)$$

$$Q_o = (H_{\text{in}} - H_{\text{out}}) \times q_o \quad (14)$$

$$\Delta \eta_{\text{cp}} = \eta_{\text{cp,r}} - \eta_{\text{cp,s}} \quad (15)$$

where B is the real-time coal feed flow rate, kg s^{-1} ; LHV is the lower heat value of the coal as fired, kJ kg^{-1} ; Q_o is the heat released by the TES system to the feedwater, kJ s^{-1} ; H_{in} is the inlet enthalpy of the heat transfer oil, kJ kg^{-1} ; H_{out} is the outlet enthalpy of Therminol VP-1, kJ kg^{-1} ; and

q_o is the flow rate of Therminol VP-1 into the oil-water heater; $\Delta\eta_{cp}$ is the whole plant thermal efficiency difference before and after coupling the TES system,%; $\eta_{cp,s}$ is the whole plant thermal efficiency before coupling the TES system,%; and $\eta_{cp,r}$ is the whole plant thermal efficiency after coupling the TES system,%. Before coupling the TES system, the Q value is 0.

2.4 Dynamic process analysis

The thermodynamic characteristics of the CFPP change and diverge from the predetermined values throughout the load-cycling dynamic processes. The "Code for an acceptance test of the modulating control system in the fossil fuel power plant"[10] states that the maximum relative deviations of the live steam pressure ($R_{p,s}$) and output power ($R_{p,w}$) of the CFPP shall not be greater than 3.0% and 2.0%, respectively.

Fig. 3 displays the output power and live steam pressure variation and relative deviation during the load increase from 30% to 50% THA at a load cycling rate of 2.2% Pe min⁻¹. The feedwater and coal flow rates rise during the loading-up process. But even when the coal feed flow rate is raised, the boiler's high thermal inertia prevents the heat from reaching the steam side of the boiler promptly. Because of this, poor performance results from delayed changes in output power and live steam pressure when the load starts to increase. Due to boiler delay, overshooting happens in both output power and live steam pressure after the loading-up procedure is finished. As observed in Fig. 3, the maximum value of $R_{p,s}$ happens during overshooting, and the maximum value of $R_{p,w}$ occurs as the load increases.

Fig. 4 illustrates that the live steam temperature setpoint (T_{ls}) remains constant at 600°C during the loading-up dynamic process, while the reheat steam temperature setpoint (T_{rh}) progressively rises from 590°C to 620°C. T_{ls} rises and then gradually decreases near the set temperature, whereas T_{rh} increases and decreases. This is because feedwater, coal, and the damper placed at the boiler's tail end are all related to T_{ls} and T_{rh} . The separator superheat is correlated with the feed coal flow rate. T_{ls} and T_{rh} rise as the load increases because the separator superheat degree is negative and the coal feed flow keeps rising.

The separator superheat progressively rises above zero as the furnace temperature rises. At this point, the feed water flow kept rising unchanged but the feed coal flow stopped rising. The opening value of the dampers fixed at the end of the boiler tail on the reheat steam side is continuously increased in order to guarantee that T_{rh}

rises from 590 °C to 620 °C. Consequently, T_{rh} continues to increase as T_{ls} decreases.

While the process of loading up is finished, the opening values of the dampers, coal feed flow rate, and feedwater flow rate progressively revert to their initial values. T_{ls} and T_{rh} eventually return to the established levels as the boiler state steadily stabilizes. T_{rh} fluctuates less and T_{ls} fluctuates more during the loading up dynamic process.

The maximum value of $R_{p,w}$ is 2.0%, the same as the maximum setting deviation value, as shown in Fig. 3. The maximum value of $R_{p,s}$ is 1.7%, significantly less than the 3.0% setting deviation value. The maximum load cycling rate for CFPP is 2.2% Pe min⁻¹ during the loading up process from 30% to 50% THA. Because $R_{p,w}$ will exceed the upper limit if the load cycling rate continues to rise. It is evident that the primary limitation of the load cycling rate of CFPP is the significant deviation brought on by the poor output power following performance.

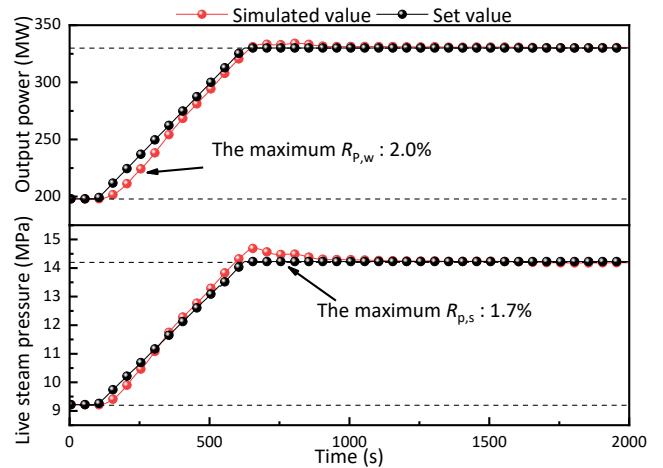


Fig. 3 Variation of output power and live steam pressure with V_e equalling 2.2% Pe min⁻¹

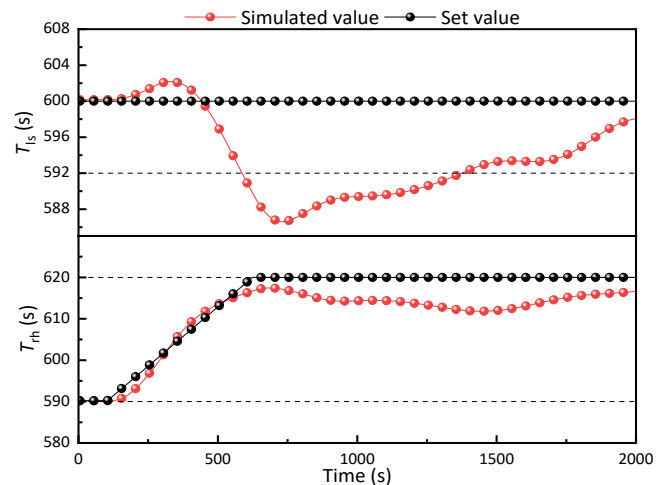


Fig. 4 Variation of T_{ls} and T_{rh} with V_e equalling 2.2% Pe min⁻¹

3. RESULTS AND DISCUSSION

It is evident from Section 2.4 that the load cycling rate is limited during the loading-up process from 30% to 50% THA. This is mostly because of the significant deviation brought on by the insufficient output power following performance. The boiler's thermal inertia is responsible for the ramp-up delay that results in insufficient output power following performance.

Therminol VP-1 transfers heat to the deaerator outlet feedwater through the oil-water heater after the TES system is coupled. This improves the insufficient output power following performance during the loading-up process and supplies extra heat to the CFPP. Thus, a coupled TES system is an excellent option for the loading up process. Therminol VP-1 flow rate and load cycling rate impact the dynamic process during loading-up from 30% THA to 50% THA is studied in this section.

3.1 Different flow rates of Therminol VP-1

3.1.1 Dynamic characteristic

The TES system couples with the CFPP to heat the feedwater during the loading-up process, and it decouples when the load reaches a set point. As illustrated in Fig. 5, coupling with the TES system results in a significant improvement in the CFPP output power following performance when compared to the original unit. However, overshooting increases, and the greatest value of $R_{p,w}$ occurs at the time of overshooting. Therminol VP-1 releases heat into the feedwater upon coupling with the TES system, hence increasing the overall heat source. Therminol VP-1 replaces part of the high extracted steam and reduces the high extracted steam flow rate, allowing more steam to reach the turbine to expand and produce power. This allows the CFPP's output power to increase quickly. The effect of increasing the output power following performance is more noticeable at greater Therminol VP-1 flow rates. Therminol VP-1 flow rate increases cause the boiler's thermal inertia to increase when the TES system is decoupled, which increases the amount of overshooting.

During the process of loading up, the TES system is coupled to heat the feedwater, and when the load reaches the set value, the TES system is decoupled. As can be seen from Fig. 5, compared with the original unit, after coupling the TES system, the output power following performance is significantly enhanced, but the overshoot increases, and the maximum value of $R_{p,w}$ occurs at the time of overshoot. This is because after coupling the TES system, Therminol VP-1 releases heat to the feedwater, providing additional heat. In addition, Therminol VP-1 replaces part of the high extraction

steam, which reduces the high extraction gas flow rate, and more steam enters the turbine to do work, prompting the output power of CFPP to rise rapidly. The higher the flow rate of Therminol VP-1, the more obvious the effect of improving the output power following performance. With the increase of the Therminol VP-1 flow rate, the thermal inertia of the boiler will be larger when the TES system is decoupled, so the overshoot will also be larger.

Before coupling the TES system, the live steam pressure fluctuates around the set value, and the maximum value of $R_{p,s}$ occurs at the time of overshooting after the completion of loading up.

After the TES system is coupled, the live steam pressure decreases compared to that before the TES system is coupled, and the maximum value of $R_{p,s}$ occurs during the loading-up process. At the end of the load rise process, the live steam pressure gradually returns to the set value. As the flow rate of Therminol VP-1 increases, the live steam pressure increases slightly, the live steam pressure following performance becomes better, $R_{p,s}$ decreases accordingly, and the time to stabilization is shortened. As can be seen from Table 3, after coupling the TES system, the maximum value of $R_{p,w}$ decreases, but the maximum value of $R_{p,s}$ increases.

Table 3 Maximum value of $R_{p,w}$ and $R_{p,s}$

Therminol VP-1 flow rate (kg s^{-1})	0	50	100	150	200
$R_{p,w}$ (%)	1.7	0.9	1.2	1.4	1.6
$R_{p,s}$ (%)	1.5	2.4	2.3	2.2	2.1

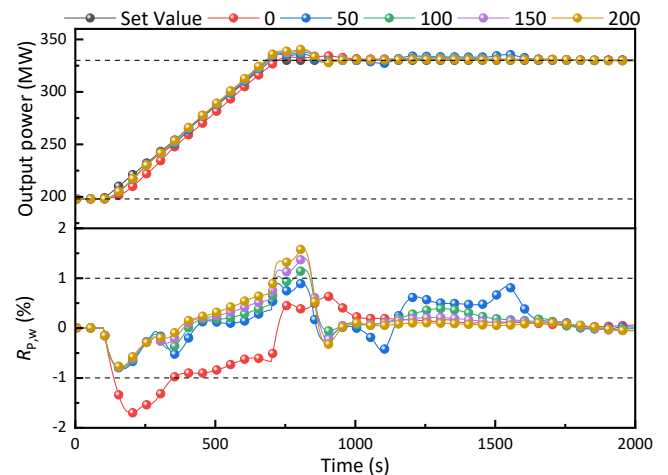


Fig. 5 Variation of output power and $R_{p,w}$ with different Therminol VP-1 flow rates

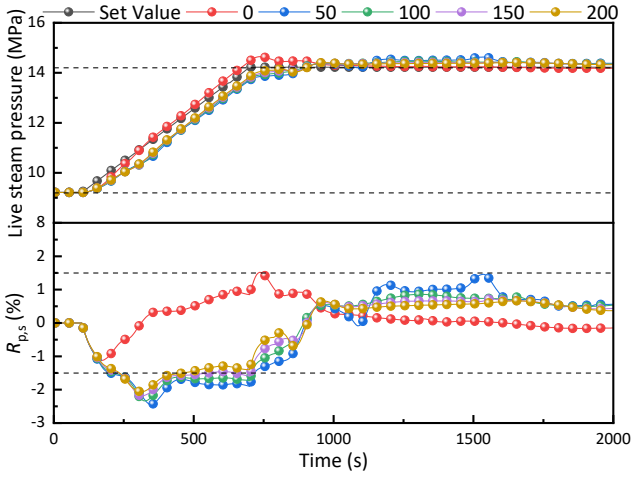


Fig. 6 Variation of live steam pressure and $R_{p,s}$ with different Therminol VP-1 flow rates

Fig. 7 shows the trends of T_{ls} and T_{rh} during the process of loading up when the Therminol VP-1 flow rates are different. It can be seen that before coupling the TES system, T_{ls} first increased slightly and then decreased, and T_{rh} fluctuated around the set temperature. After the loading-up dynamic process is completed, T_{ls} and T_{rh} gradually return to the set temperature, as detailed in Section 2.4.

After coupling the TES system, the high extraction steam is reduced, and Therminol VP-1 replaces the high extraction steam to release heat to the feedwater, providing additional heat.

For the feedwater, when the flow rate of Therminol VP-1 is low, the heat absorbed before and after coupling the TES system is basically unchanged, so the temperature of the feedwater entering the boiler is essentially the same. When the Therminol flow rate is higher, the heat absorbed by the feedwater increases and the feedwater temperature rises. As the Therminol VP-1 flow rate increases, the feedwater temperature rises and the boiler efficiency gradually decreases, offsetting the effect of the rising feedwater temperature. Before and after coupling the TES system, the feed coal flow rate inside the boiler is basically unchanged, so the T_{ls} is also basically unchanged.

After coupling the TES system, the flow rate of high extraction steam decreases and the work capacity of the HP increases. The work done steam enters the boiler is reheated to become reheated steam, so the flow of reheated steam increases. However, the amount of fuel inside the boiler is basically unchanged, so T_{rh} is lower than before coupled with the TES system. With the increase of the Therminol VP-1 flow rate, the high extraction steam flow rate continues to decrease, and the reheated steam flow rate also increases. Therefore,

T_{rh} decreases with the increase of Therminol VP-1 flow rate during the loading up process, as shown in Fig. 7.

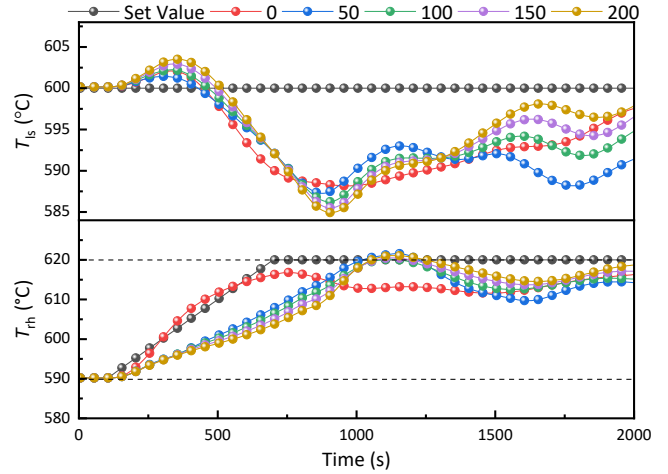


Fig. 7 Variation of T_{ls} and T_{rh} with different Therminol VP-1 flow rates

In summary, it can be seen that coupling the TES system and increasing the Therminol VP-1 flow rate are beneficial to the stability of output power, but unfavorable to the stability of live steam pressure, and have limited influence to T_{ls} and T_{rh} . However, according to Section 2.3, the main factor limiting the loading-up from 30% to 50% THA is the large deviation caused by poor output power following performance, so coupling the TES system is conducive to the stability and flexibility of CFPP.

3.1.2 Load cycling evaluation indicators

K_p is a comprehensive performance indicator that can reflect the adjustment performance quality during the load cycling process. As shown in Fig. 8, K_p is 2.46 before coupling the TES system during the 30% to 50% THA loading up process. When the Therminol VP-1 flow rate changes from 0 to 50 kg s⁻¹ after coupling the TES system, K_p increases to 2.76. Since V_e does not change, both are 2.0% Pe min⁻¹, so the ramp rate indicator K_1 is unchanged. After coupling the TES system, Therminol VP-1 releases heat to CFPP through the oil-water heater, accelerating the output power increase, thus shortening the response time and increasing K_3 . The response accuracy is less related to the above, so K_2 is almost constant. So in summary, the increase in K_p is mainly due to the increase in K_3 .

With the increase of Therminol VP-1 flow rate, K_p also increases gradually. After the Therminol VP-1 flow rate rises to 100 kg s⁻¹, K_p increases by 18.3%. When the Therminol VP-1 flow rate rises again from 100 to 200 kg s⁻¹, there is almost no change in K_p because the effect of

improving the regulatory performance by heating feedwater through Therminol VP-1 is limited.

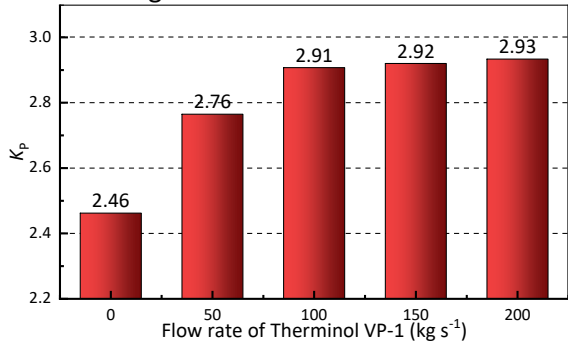


Fig. 8 K_p with different Therminol VP-1 flow rates

3.1.3 Dimensionless cumulative deviation

According to Section 3.1.1, coupled with the TES system can improve the output power following performance, and the larger the Therminol VP-1 flow rate, the better the effect. However, in response, the live steam pressure will decrease, but the increase of the Therminol VP-1 flow rate can reduce the live steam pressure drop.

Fig. 9 shows the changes of ΔP_{all} and Δp_{all} when the Therminol VP-1 flow rates are different. It can be seen that after coupling the TES system, ΔP_{all} decreases significantly, while Δp_{all} increases significantly. As the Therminol VP-1 flow rate increased from 0 to 100 kg s⁻¹, the ΔP_{all} decreased significantly. But when the Therminol VP-1 flow rate continued to increase, the ΔP_{all} remained almost unchanged. When the Therminol VP-1 flow rate was 100 kg s⁻¹, ΔP_{all} was reduced by 37.2%. The results show that the coupled TES system has a significant effect on improving the stability of the output power.

As the Therminol VP-1 flow rate increases, Δp_{all} decreases gradually. It shows that coupled the TES system can reduce the stability of live steam pressure, but increasing Therminol VP-1 flow can reduce the influence on live steam pressure.

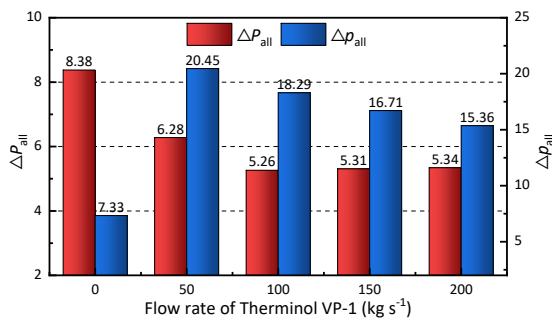


Fig. 9 ΔP_{all} and Δp_{all} with different Therminol VP-1 flow rates

3.1.4 Energy consumption analysis

From Fig. 10, it can be seen that the whole plant thermal efficiency difference ($\Delta \eta_{cp}$) decreases with increasing Therminol VP-1 flow rate and gradually changes from positive to negative after coupling the TES system during the loading up process.

This is due to the fact that when the Therminol VP-1 flow rate is low, the TES system provides additional heat to the feedwater to replace the reduced high extraction steam. The high extraction steam has a higher work capacity than the heat released by the Therminol VP-1, which effectively increases the CFPP output power and $\Delta \eta_{cp}$. When the Therminol VP-1 flow rate is higher, the TES system provides more additional heat to the feedwater, but this additional heat has less of an impact on the CFPP output power. As V_e increases, the feedwater temperature gradually rises above the setpoint and the boiler efficiency decreases, $\Delta \eta_{cp}$ with it.

When the flow rate of Therminol VP-1 is 50 kg s⁻¹, the maximum value of $\Delta \eta_{cp}$ is 0.54%; when the flow rate of Therminol VP-1 is 200 kg s⁻¹, the minimum value of $\Delta \eta_{cp}$ is -0.46%.

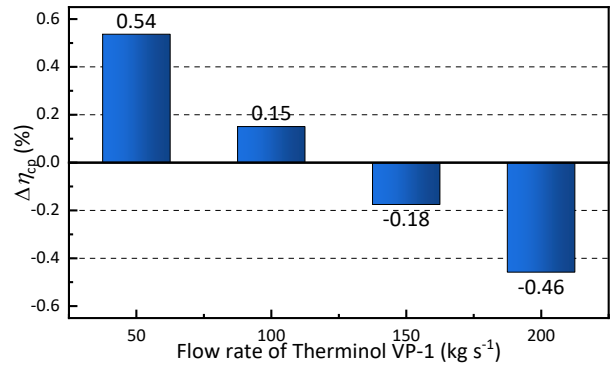


Fig. 10 $\Delta \eta_{cp}$ with different Therminol VP-1 flow rates

3.2 The maximum V_e

It can be seen from Section 3.1 that during the loading up process from 30% to 50% THA, coupling with the TES system is effective in improving the stability and flexibility of CFPP. However, the heat provided by the Therminol VP-1 to the feedwater through the oil-water heater is always limited, so this section will explore the maximum load cycling rate of CFPP at a flow rate of 100 kg s⁻¹ for Therminol VP-1.

3.2.1 Dynamic characteristic

Table 4 shows the maximum values of $R_{p,w}$ and $R_{p,s}$ of CFPP before and after coupling the TES system with V_e varying from 2.0% to 3.5% Pe min⁻¹.

For $R_{p,s}$, when V_e is 2.0%, and 2.5% Pe min⁻¹, coupling the TES system is not conducive to reducing $R_{p,s}$. When

V_e is $3.0\% \text{ Pe min}^{-1}$, $R_{p,s}$ does not change after coupling the TES system. When V_e is $3.5\% \text{ Pe min}^{-1}$, coupled with the TES system helps to reduce $R_{p,s}$ and increase V_e . However, no matter whether the TES system is coupled or not, $R_{p,s}$ is less than 3.0% , which meets the requirement.

Since $R_{p,s}$ all meet the requirements, our focus is on the reduction of $R_{p,w}$. Fig. 11 shows the changes of $R_{p,w}$ before and after coupling the TES system when V_e ranges from 2.0% to $3.5\% \text{ Pe min}^{-1}$. It can be seen that the maximum value of $R_{p,w}$ all appears in the stage of loading up, and all exceed 2.0% . After coupling the TES system, the $R_{p,w}$ of CFPP decreases obviously, and all of them are less than 2.0% . After coupling the TES system, when V_e is $2.0\% \text{ Pe min}^{-1}$, $R_{p,w}$ is minimally reduced by 11.8% ; when V_e is $3.0\% \text{ Pe min}^{-1}$, $R_{p,w}$ is maximally reduced by 26.7% . It can be seen that coupled with the TES system is very effective in improving the following performance of the output power during the loading up process, and after the load cycling process is completed, the overshoot of the output power is very small. When V_e is $3.5\% \text{ Pe min}^{-1}$, $R_{p,w}$ has reached 1.9% , very close to the limit value of 2.0% , so we can show that when the flow rate of Therminol VP-1 is 100 kg s^{-1} , the maximum value of V_e can be increased from 2.2% to $3.5\% \text{ Pe min}^{-1}$.

Therefore, we can conclude that coupling the TES system with Therminol VP-1 as the heat transfer fluid is very effective for improving flexibility and stability during the dynamic process from 30% to 50% THA. The maximum value of the V_e can be increased from 2.2% to $3.5\% \text{ Pe min}^{-1}$.

Table 4 Maximum value of $R_{p,w}$ and $R_{p,s}$

V_e ($\% \text{ Pe min}^{-1}$)	2.0	2.5	3.0	3.5
$R_{p,w}$ (%)	1.7	2.3	3.0	3.8
$R_{p,w}$ (%) (Coupled TES)	1.2	1.2	1.5	1.9
$R_{p,s}$ (%)	1.5	1.9	2.2	2.9
$R_{p,s}$ (%) (Coupled TES)	2.3	2.2	2.2	2.2

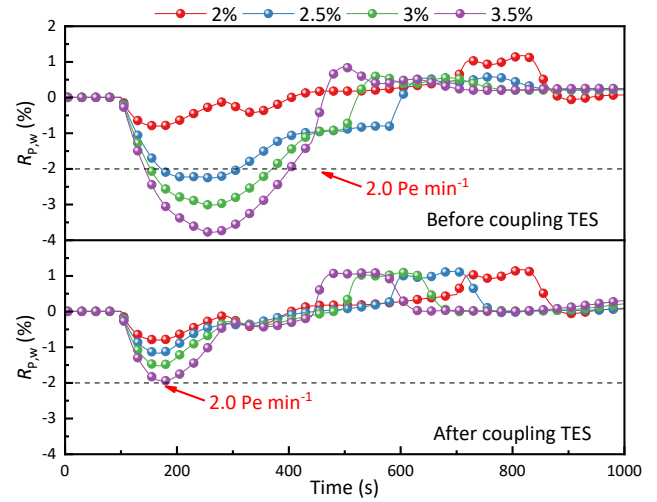


Fig. 11 $R_{p,w}$ before and after being coupled with the TES system with different V_e

3.2.2 Load cycling evaluation indicators

Fig. 12 shows the variation of K_p under different load cycling rates before and after coupling the TES system. Before coupling the TES system, the ramp rate indicator K_1 increases with the increase of V_e . K_2 has little relationship with V_e and, therefore, hardly changes. With the increase of V_e , the variation ranges of CFPP feedwater and coal feed supply are also larger, so the time for output power to start responding is also shortened, and K_3 increases. Thus, the increase in K_p is mainly due to the increase in K_1 and K_3 .

According to Section 3.1.2, the increase in K_p after coupling the TES system is due to the increase in the response time indicator K_3 . Thus, coupling the TES system is an effective way to increase K_p even in the V_e rang from 2.0% to $3.5\% \text{ Pe min}^{-1}$, which is also proved in Fig. 12.

After coupling the TES system, VP-1 provides additional heat to the CFPP, thus promoting a rapid increase in output power and shortening the response time of output power. The larger the V_e , the more additional heat is required during the loading-up process. Since the Therminol VP-1 flow rate is constant, the real-time heat supplied by Therminol VP-1 to the CFPP is almost constant when coupled with the TES system. The larger the V_e , the smaller the proportion of heat supplied by Therminol VP-1 to that required by the CFPP. Therefore, as V_e increases, the lifting effect of K_p becomes smaller. When V_e is $2.0\% \text{ Pe min}^{-1}$, K_p increases by a maximum of 24.5% after coupling the TES system, while when V_e is $3.5\% \text{ Pe min}^{-1}$, K_p increases by 15.3% .

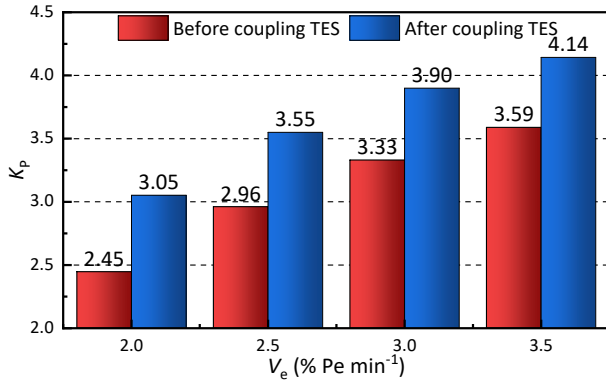


Fig. 12 K_p before and after being coupled with the TES system with different V_e

3.2.3 Dimensionless cumulative deviation

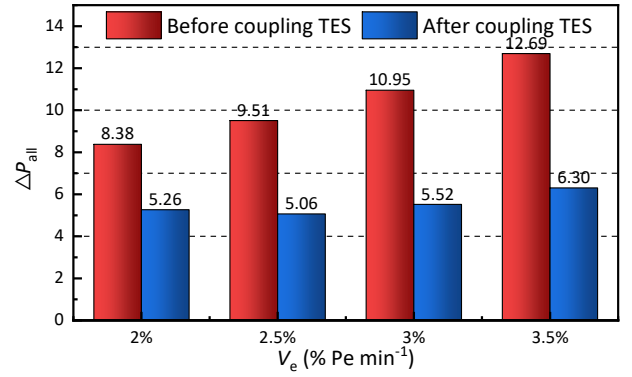
As illustrated in Section 3.1.3, coupling with the TES system has a good effect on improving the stability of the output power but is not conducive to the stability of the live steam pressure. Fig. 13 shows ΔP_{all} and Δp_{all} under different V_e before and after coupling the TES system.

Before coupling the TES system, with the increase of V_e , the change of boiler state is accelerated, and the fluctuation of output power and live steam pressure during the process of loading up is also increased. Therefore, ΔP_{all} and Δp_{all} increase with the increase of V_e , which is not conducive to the stability of the loading up dynamic process.

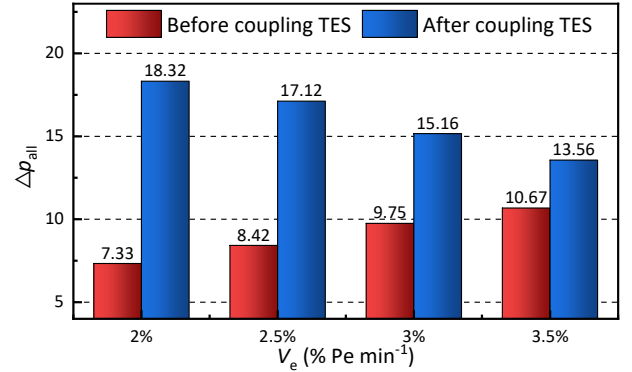
After coupling the TES system, ΔP_{all} decreases significantly due to the improvement of output power following performance. Since the V_e of CFPP itself can only reach 2.2% Pe min⁻¹, the larger the V_e , the more difficult it is for CFPP to carry out the load cycling process. Coupled with the TES system can increase the stability of the output power, so as to achieve higher V_e . The larger the V_e , the more helpful the TES system will be to CFPP during the load cycling process. Therefore, it can be seen from Fig. 13 (a) that when V_e is 3.5% Pe min⁻¹, ΔP_{all} can be reduced by 50.4% at most. When V_e is 2.0% Pe min⁻¹, ΔP_{all} can be reduced by 37.2% at least.

As shown in Fig. 13 (b), with the increase of V_e , the shorter the time of coupling the TES system, the less the influence on the live steam pressure, so the Δp_{all} gradually decreases. Before coupling the TES system, Δp_{all} increases with the increase of V_e , so the influence of coupling the TES system on Δp_{all} decreases gradually.

In summary, in the case of large V_e , coupled with the TES system plays a more obvious role in improving the flexibility and stability of CFPP.



(a) ΔP_{all}



(b) Δp_{all}

Fig. 13 ΔP_{all} and Δp_{all} before and after being coupled with the TES system with different V_e

3.2.4 Energy consumption analysis

From section 3.1.4, it can be seen that the output power of CFPP can be effectively enhanced when the Therminol VP-1 flow rate is low and $\Delta \eta_{cp}$ is greater than zero. From Fig. 14, it can be seen that $\Delta \eta_{cp}$ is greater than zero when V_e is in the interval segment from 2.0 to 3.5% Pe min⁻¹, which indicates that Therminol VP-1 flow rate of 100 kg s⁻¹ is able to effectively enhance the output power of CFPP.

As V_e gradually increases, $\Delta \eta_{cp}$ gradually decreases. This is due to the fact that the TES system is coupled only when the load rises, and when the load rises ends, the TES system decouples. As V_e gradually rises, the duration of the load rise period decreases, the less additional heat is provided by the TES system, the economic impact on the overall variable load process decreases, and therefore $\Delta \eta_{cp}$ decreases.

When the Therminol VP-1 flow rate is 100 kg s⁻¹, $\Delta \eta_{cp}$ has a maximum of 0.15% at V_e of 2.0% Pe min⁻¹ and a minimum of 0.02% at V_e of 3.5% Pe min⁻¹.

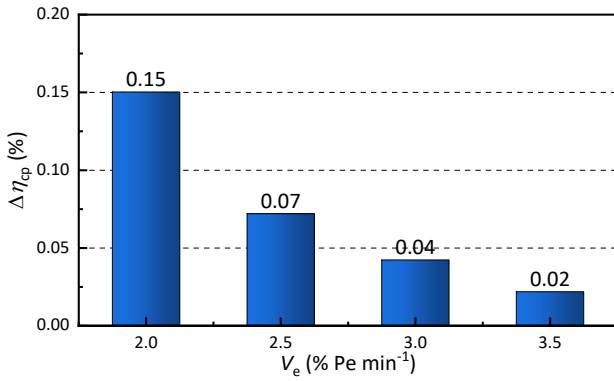


Fig. 14 $\Delta\eta_{cp}$ before and after being coupled with the TES system with different V_e

4. CONCLUSION

In this paper, a thermal energy storage system with Therminol VP-1 as thermal oil is coupled, and the dynamic characteristics of CFPP from 30% to 50% THA under different conditions are discussed. The conclusion of this paper is as follows:

(1) When the flow rate of Therminol VP-1 is 100 kg s^{-1} , the flexibility of the coal-fired power plant can be effectively increased, and the maximum value of the load cycling rate can increase from 2.2% to $3.5\% \text{ Pe min}^{-1}$.

(2) The main limiting factor to the flexibility of coal-fired power plants is the large output power fluctuations. At a load cycling rate of $2.0\% \text{ Pe min}^{-1}$ and a Therminol VP-1 flow rate of 100 kg s^{-1} , the coupled thermal storage system reduces the maximum relative deviation of the output power $R_{P,w}$ by 11.8%, improves the overall performance index K_P by 18.3%, and reduces the cumulative deviation of the dimensionless output power ΔP_{all} by 37.2%.

(3) When the load cycling rate is $2.0\% \text{ Pe min}^{-1}$, the whole plant thermal efficiency difference $\Delta\eta_{cp}$ is gradually reduced from 0.54% to -0.46% as the VP-1 flow rate is raised from 50 to 200 kg s^{-1} . When the VP-1 flow rate is 100 kg s^{-1} , the whole plant thermal efficiency difference gradually decreases from 0.15% to 0.02% as V_e is raised from 2.0% to $3.5\% \text{ Pe min}^{-1}$, but all are positive.

ACKNOWLEDGEMENT

This work was supported by the National Key R&D Program of China (Grant Number 2022YFB4100401).

REFERENCE

[1]GU Y, XU J, CHEN D, et al. Overall review of peak shaving for coal-fired power units in China [J]. Renewable & Sustainable Energy Reviews, 2016, 54: 723-31.

[2]WANG Y, LIU Y, LI X, et al. GORFLM: Globally Optimal Robust Fitting for Linear Model [J]. Signal Processing-Image Communication, 2020, 84.

[3]ZHANG K, LIU M, ZHAO Y, et al. Design and performance evaluation of a new thermal energy storage system integrated within a coal-fired power plant [J]. Journal of Energy Storage, 2022, 50.

[4]LI D, WANG J. Study of supercritical power plant integration with high temperature thermal energy storage for flexible operation [J]. Journal of Energy Storage, 2018, 20: 140-52.

[5]TROJAN M, TALER D, DZIERWA P, et al. The use of pressure hot water storage tanks to improve the energy flexibility of the steam power unit [J]. Energy, 2019, 173: 926-36.

[6]DING H, DING S, TAN Q, et al. Improving power ramp rate of a coal-fired power plant by a bypass steam accumulator [J]. Heliyon, 2024, 10(11).

[7]PEIRO G, GASIA J, MIRO L, et al. Influence of the heat transfer fluid in a CSP plant molten salts charging process [J]. Renewable Energy, 2017, 113: 148-58.

[8]ABED N, AFGAN I, CIONCOLINI A, et al. Assessment and Evaluation of the Thermal Performance of Various Working Fluids in Parabolic Trough Collectors of Solar Thermal Power Plants under Non-Uniform Heat Flux Distribution Conditions [J]. Energies, 2020, 13(15).

[9]BENOIT H, SPREAFICO L, GAUTHIER D, et al. Review of heat transfer fluids in tube-receivers used in concentrating solar thermal systems: Properties and heat transfer coefficients [J]. Renewable & Sustainable Energy Reviews, 2016, 55: 298-315.

[10] Zhejiang electric power Test and Research Institute. Code for a acceptance test of modulating control system in the fossil fuel power plant [Z]. Industry standard - Electricity. 2006: 19P.A4